International Journal of Hydrogen Energy 100 (2025) 749–759

Contents lists available at ScienceDirect

International Journal of Hydrogen Energy

journal homepage: www.elsevier.com/locate/he

# Economic optimization for the dynamic operation of a grid connected and battery-supported electrolyzer

Patrick Mößle [a,c,*,1], Tim Herrmannsdörfer [b,c,1], Matthias Welzl [b,c], Dieter Brüggemann [b,c], Michael A. Danzer [a,c]

[a] University of Bayreuth, Chair for Electrical Energy Systems (EES), Universitätsstraße 30, 95447 Bayreuth, Germany
[b] University of Bayreuth, Chair of Engineering Thermodynamics and Transport Processes (LTTT), Universitätsstraße 30, 95447 Bayreuth, Germany
[c] Center of Energy Technology (ZET), Prof. Rüdiger-Bormann-Straße 1, 95447 Bayreuth, Germany

ARTICLE INFO

*Keywords:*
Optimization
Grid connected electrolyzer
Battery energy storage
Aging model
Operating strategy

ABSTRACT

Proton exchange membrane electrolyzers (PEMEL) are considered a promising technology for intermittent generation of green hydrogen if connected to fluctuating energy sources and in volatile electricity markets. For an economic operation, a coupling of PEMEL with a battery energy storage system (BESS) is advantageous. In this work, optimized operating strategies of a grid connected PEMEL supported by a BESS are developed based on dynamic programming. Furthermore, a generic aging model is implemented to ensure that performance degradation is taken into account. The optimization is carried out for different hydrogen production targets per week based on day-ahead market electricity prices, system configurations with and without combined operation of electrolyzer and battery as well as aging effects. The results show that an optimized operating strategy can decrease the effective operating costs, i.e. electricity procurement costs and costs related to system degradation, of the considered use case by up to 7 %.

## 1. Introduction

### 1.1. Motivation

Hydrogen is considered as one of the key elements for sector coupling in future energy systems. Due to its wide range of possible applications, it can contribute to the decarbonization of the electricity, heating, mobility as well as industrial sector [1]. As a result, the global hydrogen demand will increase rapidly [2]. Among the various electrolyzer (El) technologies, the PEM electrolyzer (PEMEL) is a promising option for intermittent operation [3–7]. The main advantages of PEMEL in terms of dynamic operation are a high load flexibility and fast response times [7–9] as well as fast start-up times [7,10,11]. This enables coupling with fluctuating energy sources such as solar and wind, as well as direct connection to the electricity grid to benefit from dynamic electricity prices [10]. An example of a large-scale grid connected PEMEL plant is located in Wunsiedel, a town in northern Bavaria. It is one of Germany's largest electrolyzer plants in operation with an electrical power of 8.75 MW. This corresponds to a maximum annual hydrogen production of 1,350 t.

### 1.2. Literature review

To operate grid connected electrolyzers economically, optimized operating strategies are essential to compete with hydrogen from fossil fuels, such as steam reforming of natural gas or coal gasification. Various studies have already investigated different operating strategies for grid connected electrolyzers. Kopp et al. [12] evaluated the electricity procurement for a 6 MW PEMEL at the "Energiepark Mainz" in Germany. The results show that participation in the secondary control reserve is the most profitable option in terms of electricity procurement costs (EPC). The electricity procurement for five Canadian provinces using flat-rate prices and real-time prices for the wholesale markets in Germany, California and Ontario was analyzed by Nguyen et al. [10]. In their study they developed an operating strategy, that can reduce the electricity costs of grid connected electrolyzers in Germany by 4–9 %. Jørgensen and Ropenus [13] calculated the hydrogen production price of grid connected electrolyzers in the West Danish power market area. The authors conclude that a more flexible operation of the electrolyzer by reducing the operating hours does not necessarily lead to a significant reduction in the hydrogen production price. Using Monte Carlo simulations for grid connected electrolyzers at the Danish

* Corresponding author at: University of Bayreuth, Chair for Electrical Energy Systems (EES), Universitätsstraße 30, 95447 Bayreuth, Germany.
*E-mail address:* patrick.moessle@uni-bayreuth.de (P. Mößle).
[1] Authors contributed equally.

https://doi.org/10.1016/j.ijhydene.2024.12.216
Received 18 September 2024; Received in revised form 9 December 2024; Accepted 12 December 2024
Available online 26 December 2024

electricity market, Ghaebi Panah et al. [14] were able to show that both PEMEL and alkaline electrolyzers (AEL) can already achieve hydrogen production costs of less than 3 € $kg^{-1}$ assuming that taxes and levies are neglected.

As special feature besides the electrolyzer, one of the largest battery energy storage systems (BESS) in Bavaria with a total capacity of 10.3 MWh (usable 9 MWh) is located at the Wunsiedel Energy Park. This enables the implementation of a coupled operating strategy of electrolyzer and BESS, which can provide additional flexibility for the local hydrogen production. Many studies have already focused on hybrid systems of electrolyzers and batteries. Papadopoulos et al. [15] attempted to increase the utilization factor of a PEMEL through various hybrid system designs by combining photovoltaics and wind power with BESS. The results show that although the utilization factor can be increased by using BESS, the high investment costs lead to increased payback periods. The work by Gillessen et al. [16] demonstrates that batteries can be used to support the operation of electrolyzers directly connected with PV plants. From an economic point of view, though, it is more profitable to increase the electrolyzer capacity than to invest in an additional BESS. In the presented studies, degradation phenomena of electrolyzer and BESS are neglected. However, the aging of electrolyzer plants in dynamic operation is currently a major issue [6,17]. The work of Wallnöfer-Ogris et al. [18] provides a broad overview of the degradation mechanisms and their underlying influencing factors within a PEMEL. There are only a few studies in literature that examine operating strategies considering electrolyzer aging. Parra and Patel [19] developed a dynamic power-to-gas (PtG) model regarding electrolyzer aging to calculate the performance and levelized cost of the plant. Aging was integrated into the model using a constant voltage increase of 2 μV $h^{-1}$ for AEL and 5 μV $h^{-1}$ for PEMEL. Matute et al. [20] developed a techno-economic model to calculate the optimal hourly operation of grid connected electrolyzers for the production of hydrogen for different end-use applications. A maximum number of cold starts as well as a constant hourly stack replacement costs have been defined for aging considerations. The aging of the BESS also plays an important role in a coupled operating strategy. Torreglosa et al. [21] and García et al. [22] have defined a minimum state-of-charge (SOC) for the BESS in order to avoid total discharges of the battery and thus increase its lifetime. This approach was also followed in the work of Zhao et al. [6], in which a multi-objective energy dispatch strategy for a hybrid energy storage system was developed to achieve cost-effective hydrogen production and long-life operation. The aging of the electrolyzer is not quantified directly, but is considered indirectly using a defined volatility indicator. The combination of electrolyzer and battery reduces the volatility indicator of the electrolyzer by 49 % as it is no longer used to compensate the frequently occurring power fluctuations of renewable energy generation. Zhou et al. [23] investigated the techno-economic-environmental performance of a hybrid $H_2$-BESS for different cases. In addition, dynamic degradation models were developed for both the battery and the fuel cell, and the influence of different operating strategies on component aging was studied. Another hybrid system consisting of an off-grid AEL system integrated with solar and wind power as well as a BESS was analyzed by Ibáñez-Rioja et al. [24]. The objective of their work was to simultaneously optimize component capacities, system control as well as to minimize the levelized cost of hydrogen considering component degradation and replacements during operation. Maluenda et al. [25] developed a chance-constrained stochastic model for a PV–BESS–Electrolyzer system that can participate in different energy markets. By implementing a detailed degradation model for the BESS, a more accurate assessment of operating costs was achieved. For a comparison with this work, a selection of the literature presented that also optimize operating strategies is given in Table 1.

### 1.3. Research gap and scientific significance

To the best of the authors' knowledge, no optimization algorithms for a system with coupled operation of a grid connected electrolyzer and a BESS considering aging as a function of the operating point can be found in literature. Most optimization approaches do not specifically aim at operating strategies that minimize component degradation due to undesirable operating points. They rather include aging models to quantify the degradation effects of certain operating scenarios. To consider component degradation in the optimization of the operating strategy, a mathematical model is required that can be implemented in the objective function of the algorithm. Thus, a quantification of aging depending on the operating conditions is needed that can be expressed in a monetary value to be minimized by the algorithm. Most studies also do not optimize the operating strategy under the constraint of a specified hydrogen production target. Hydrogen production is typically aligned with the production profiles of renewable energy sources. However, many plant operators need to reach a certain target amount of hydrogen to meet the demand of their customers. In this work an algorithm based on dynamic programming (DP) is developed to solve such an optimization problem for hybrid hydrogen production systems and simultaneously minimize EPC and component degradation. Due to the strict constraint of a weekly hydrogen production target, this enables the application for plant operators who are bound to time-sensitive supply contracts. The flexibility of the combination of DP as well as of the introduced aging models leads to a wide range of applicability of the algorithm. It can easily be used for different electrolyzer and BESS technologies as well as different scenarios and desired target values.

In the following the main contributions of this paper are summarized briefly.

(1) The optimization algorithm is able to provide the optimal operating strategy of the hybrid hydrogen production system based on an existing plant for various scenarios. These include different hydrogen production targets, coupled strategies with BESS and component aging considerations.
(2) The resulting globally optimal solutions for each scenario provide a benchmark for system operators in their decision-making process regarding plant scheduling.
(3) The flexibility of the algorithm allows not only to optimize a strategy for minimized EPC and aging, but also to focus on only one of the two.

The working principle is presented for the grid connected PEMEL and the BESS at the Wunsiedel Energy Park, where electrical energy can be provided as well as consumed. The outline of this paper is structured as follows. In Section 2 the overall optimization problem is formulated and the working principle of the optimization algorithm is explained. Section 3 shows how the models are adopted to the example of the Wunsiedel Energy Park, while Section 4 documents in detail how the mentioned example is implemented into the algorithm. In Section 5 the exact scenarios with the respective constraints and the sensitivity analysis for the simulation are listed. The corresponding results are shown in Section 6, followed by the summary in Section 7.

## 2. Definition and solution of the optimization problem

The overall objective of the developed algorithm is to calculate the globally optimal operating strategy that minimizes the effective operating costs (EOC) of a hybrid hydrogen production system with a secondary energy storage. The algorithm is applicable to all grid-connected electrolyzer and battery technologies. Additionally, the optimization input can be electricity prices from any power market, e.g. intraday or day-ahead. The desired target value for the production and the simulated observation period of the optimized operating strategy can also be chosen freely. Implementation of component degradation into the decision process calls for a suitable aging model that translates harmful operating conditions into a monetary value. Further information on the aging model can be found in Section 2.3.

**Table 1**
Categorization of selected literature indicating system modeling (M) of electrolyzer and BESS, consideration of component aging (A), aging implementation and optimization result.

| Authors (alphabetical) | El | BESS | Aging implementation | Optimization result |
|---|---|---|---|---|
| Gillessen et al. [16] | M | M | – | Operating strategy for off-grid El + BESS without specified hydrogen demand |
| Ibáñez-Rioja et al. [24] | M + A | M + A | BESS: Cyclic + calendar aging<br>El: Constant efficiency decrease | Operating strategy for off-grid El + BESS without specified hydrogen demand |
| Maluenda et al. [25] | M | M + A | BESS: Cyclic aging | Operating strategy for off-grid El + BESS without specified hydrogen demand |
| Matute et al. 1 [20] | M + A | – | El: Max. number of cold starts + hourly stack replacement costs | Operating strategy for grid-connected El with specified weekly hydrogen demand |
| Parra and Patel [19] | M + A | – | El: Constant voltage increase | Profitability of a grid-connected electrolyzer without specified hydrogen demand |
| Zhao et al. [6] | M + A | M + A | BESS: SOC operating limits<br>El: Volatility indicator | Operating strategy for off-grid El + BESS without specified hydrogen demand |

### 2.1. Problem definition

According to the mentioned framework the optimization problem can be characterized as follows. The problem

1. needs to be solved for one specific target value and a predefined time interval,
2. is a minimization of costs,
3. is constrained by the boundary conditions of the system such as power or capacity limits,
4. is sequential due to the time series of electricity prices,
5. is solved to provide a global optimum.

### 2.2. Dynamic programming

Dynamic programming is an appropriate choice to solve this optimization problem. An alternative to DP pose multi-objective optimization [26,27] or mixed integer linear programming [28]. Since the economic optimum of the plant operation is of interest in this work, DP is identified as the ideal option as it always ensures the global optimum [29].

The concept of DP results from Richard Bellman's principle of optimality that involves breaking down complex problems into smaller subproblems and solving them recursively to determine an overall solution. Therefore, the optimal solution to a trajectory problem can be constructed from the optimal solutions of its partial trajectories [30,31]. Consequently, DP provides a way to solve problems that would be intractable using brute force or exhaustive search methods by efficiently reusing solutions to subproblems multiple times [32–34]. Due to the sequential nature of the scenario that is optimized, those subproblems are solved at every time step.

Similar to other optimization algorithms an objective function

$$F(x_1, \ldots, x_n) = \sum_{k=1}^{N} f_k(z_{k-1}, x_k) \tag{2.1}$$

is minimized by the DP. The objective function $f_k$ for each specific subproblem is calculated for all time steps $k$ within the simulated time period $N$. As $f_k$ only is dependent on the states of the last time step $z_{k-1}$ and the decision of the current time step $x_k$, the objective function is not related to any later states of the system. Therefore, the Markov property is met, which is a prerequisite for DP [32,35,36]. Cormen [37] describes techniques such as memoization (top-down) or tabulation (bottom-up) that are employed to store and reuse computed subproblem solutions. Memoization is a technique to optimize the computation of subproblems by storing their solutions for future reference. It involves keeping a record (memo) of the solutions to previously solved subproblems so that they can be directly accessed instead of being recomputed. When a subproblem needs to be solved, memoization first checks if its solution is already available in the memo. If it is, the stored solution is retrieved, eliminating the need for redundant calculations. If the solution is not present, the subproblem is solved, and its solution is stored in the memo for future use. It is a key technique in optimizing the efficiency of DP solutions.

Additionally, the transfer function $t_k(z_{k-1}, x_k)$ determines the state $z_k$ at the current time step. The decision space $X_k$ and the state space $Z_k$ define the limits of $x_k$ and $z_k$. More details on the objective function, decision and state space for the specific optimization problem in this paper are presented in Section 4. The initial state $z_0$ and the final state $z_N$ can be predefined, but are fixed values during optimization [32,35]. For the purpose of this paper $z_0$ is always defined as 0. Therefore, the following equations and conditions can be formulated:

$$x_k \in X_k(z_{k-1}); \tag{2.2}$$

$$z_k \in Z_k; \tag{2.3}$$

$$z_0 = 0; \tag{2.4}$$

$$z_{\text{end}} = z_N; \tag{2.5}$$

$$z_k = t_k(z_{k-1}, x_k). \tag{2.6}$$

Depending on the number of states at the initial or the final step, DP can be evaluated by forward or backward recursion. Forward recursion is preferred when there are restrictions on the initial state space, backward recursion, when a fixed target needs to be met [29].

Numerous real-world problems, ranging from computer algorithms [38] and resource allocation [36,39] to economics (portfolio optimization, production planning, and optimal taxation) [40], have benefited from the application of DP.

However, this algorithm also has some limitations and potential disadvantages, like dividing complex problems into suitable subproblems [37] or significant memory and computing time requirements. The space complexity of DP algorithms can also be a limitation in certain scenarios [41].

### 2.3. Generic aging model

The aging model must reflect the component aging mechanisms as a function of the operating point. Therefore, a generic, universally applicable aging model is developed that allows to quantify the service lifetime of a plant in an economic value. The specific aging costs

$$c_{QLV} = \frac{CAPEX}{QLV} \tag{2.7}$$

are defined as capital expenditures ($CAPEX$) divided by the expected system lifetime expressed in the quantified lifetime variable ($QLV$). This way, the $CAPEX$ are integrated in the operating costs resulting from system degradation. The definition of $QLV$ can be adjusted to the modeled system (see Sections 3.2 and 3.3). Depending on the considered system, harmful operating conditions and boundaries of the generic model can be defined in a function $g$. This function determines

the influence of operating points and system states on the aging of the specific plant in form of aging factors $F_{\text{aging}}$ and result in additional $QLV$. In combination with $c_{QLV}$ the degradation costs

$$C_{\text{aging}} = g(F_{\text{aging}}) \cdot c_{QLV} \tag{2.8}$$

resulting from the additional $QLV$ can be calculated.

## 3. Proof of concept

### 3.1. Adaption of the problem definition

The functionality of the optimization algorithm developed to solve the problem described in Section 2 is shown for the example of Wunsiedel Energy Park. In this use case the EPC are reduced by implementing the BESS into the optimization process of the operating strategy to support the economic profitability of the grid connected electrolyzer. The optimization of the EOC not only minimizes the EPC, but also reduces harmful operating strategies for both the electrolyzer and the BESS to prevent premature aging due to degradation of the components. This combined approach, opens up completely new possibilities for operating the PEMEL. The integration of the BESS enables the PEMEL to produce hydrogen more economically considering the electricity market, since energy can be stored within the BESS at low prices and be used to supply the electrolyzer at high prices. Full knowledge of the electricity prices of the day-ahead market with different values on an hourly basis for one week is assumed. This time horizon represents a realistic horizon for electricity price forecasts that system operators need to use during their planning of their operating strategy [42]. Therefore, for each electricity price a decision must be made about the operating strategy of the electrolyzer. Additionally, whenever the electrolyzer produces hydrogen, the source of the power supply for its operation has to be determined. It can be powered by the grid, the BESS or partly by both. To supply the electrolyzer with electrical energy, an hourly decision must also be made as to whether the BESS should be charged, discharged or left idle. The maximum power and the corresponding hydrogen production are limited by the electrolyzer. Similarly, the maximum charging and discharging power of the BESS is restricted by the system itself and depends on the state of energy ($SOE$) and the maximum energy that can be stored in the BESS. The production target represents a variable that is defined weekly by the plant operators and thus represents a fixed target value for the optimization that must be fulfilled. Consequently, the algorithm executes simulations for every week of the year.

Corresponding to Section 2, the specific constraints for the use case can be expressed as follows.

1. The hydrogen mass that has to be produced for one week is a fixed value.
2. EOC consisting of EPC and costs related to aging are minimized during optimization.
3. System limitations are the power of the PEMEL and the BESS and the storage capacity of the BESS.
4. Due to new electricity prices at every hour from the day-ahead market the problem is sequential.
5. The aim is to find the best economical solution (global optimum) for the operating strategy to assist plant operators in their decision making.

Models that simulate the behavior of the systems involved need to be designed for the optimization additionally to the degradation model. In Fig. 1 the schematic representation of the overall system can be seen. The PEMEL and BESS models are simplified to avoid a considerable increase in computing time and do not include downstream processes such as hydrogen storage and compression.

The boundaries and conditions in this paper are chosen by the authors based on the plants at Wunsiedel Energy Park to demonstrate the practicality of the algorithm. Those values can be adapted to different typologies and technologies. The developed simulation models are described in more detail in the following sections.

### 3.2. Electrolyzer

The electrolyzer model is divided into two sub-models. The first sub-model is used to determine the amount of hydrogen produced depending on the given operating point. The study by Kopp et al. [12] shows the hydrogen production of a PEMEL plant as a function of the total power consumption. The data illustrate an almost linear relationship between hydrogen production and the required power input. The PEMEL in Wunsiedel has a minimum operating power of approximately 20 % of its maximum power. The assumption of a linear relationship is further supported by the work of Kopp et al. where the input power is considered to be always higher than 20 %. For this purpose, a linear relation between hydrogen production ($\dot{m}_{\text{H2,max}} = 165\,\text{kg}\,\text{h}^{-1}$) and the electrical power consumption of the electrolyzer is considered in terms of the factor $\beta_{\text{P2M}}$ (see Eq. (4.1)) in this work. In the second part of the model, the aging of the electrolyzer has to be quantified. The aging submodel is based on Eq. ((2.7) and (2.8)). In case of Wunsiedel, the $QLV$ of the electrolyzer is specified in equivalent operating hours (EOH). Compared to full load hours (FLH), EOH also consider the aging of the electrolyzer depending on the operating conditions. According to the manufacturer, the system reaches the end of lifetime after 80,000 EOH. During the dynamic operation of an electrolyzer several conditions occur that have a negative impact on aging phenomena. In addition to the operating point itself, these also include the load gradients between different time steps and start-stop sequences. In the aging model, various factors are assigned to the different conditions, which are expressed in form of EOH (see Table 2).

**Table 2**
Critical operating conditions for the aging of the electrolyzer.

| Factor | Operating condition | Value in EOH |
|---|---|---|
| $F_{\text{s}}$ | Start-stop | 1.0[a] |
| $F_{\text{o}}$ | $P_{\text{El}} = 0\ \%\ P_{\text{max}}$ | 0.1[a] |
| | $P_{\text{El}} <= 40\ \%\ P_{\text{max}}$ | 1.5[a] |
| | $40\ \%\ P_{\text{max}} < P_{\text{El}} < 80\ \%\ P_{\text{max}}$ | 1.0[a] |
| | $P_{\text{El}} > 80\ \%\ P_{\text{max}}$ | 1.2 |
| $F_{\text{g}}$ | Load gradient | $0.05 \cdot \frac{\Delta P}{\text{MW}}$ |

[a] Values according to the manufacturer.

According to the manufacturer, operating the electrolyzer at less than 40 % of the maximum power results in a higher number of EOH. There is also an aging process considered even when the system is not operating. For operation above 40 % the manufacturer has defined a fixed EOH value of 1. In addition, each start-stop sequence is credited with a further EOH. This type of degradation modeling is also applied in the real plant on site. At high power, the resulting high current density leads to an increase in ohmic losses and thus to considerable thermal stress on the cell [4,43]. Therefore, in addition to the manufacturer's specifications an increased aging factor is also assumed for operating points higher than 80 %. For the influence of the load gradient, a linear dependence on the resulting number of EOH is assumed in this work. Along with the $CAPEX$ for an electrolyzer stack and Eq. (2.7) the costs per EOH ($c_{\text{EOH}}$) can be determined (see Table 6). Thus, the costs arising from the aging of the electrolyzer

$$C_{\text{aging,El}} = \left( \sum_{i=1}^{N_{\text{s}}} F_{\text{s},i} + \sum_{j=1}^{N_{\text{o}}} (F_{\text{o},j} + F_{\text{g},j}) \right) \cdot c_{\text{EOH}} \tag{3.1}$$

are calculated under consideration of the respective operating conditions. Here, $F_{\text{s}}$, $F_{\text{o}}$ and $F_{\text{g}}$ indicate the factors for start-stop sequences, operating points in form of the electrical input power and load gradients in EOH and can be found in Table 2. $N_{\text{s}}$ and $N_{\text{o}}$ represent the numbers of starts and operating points.

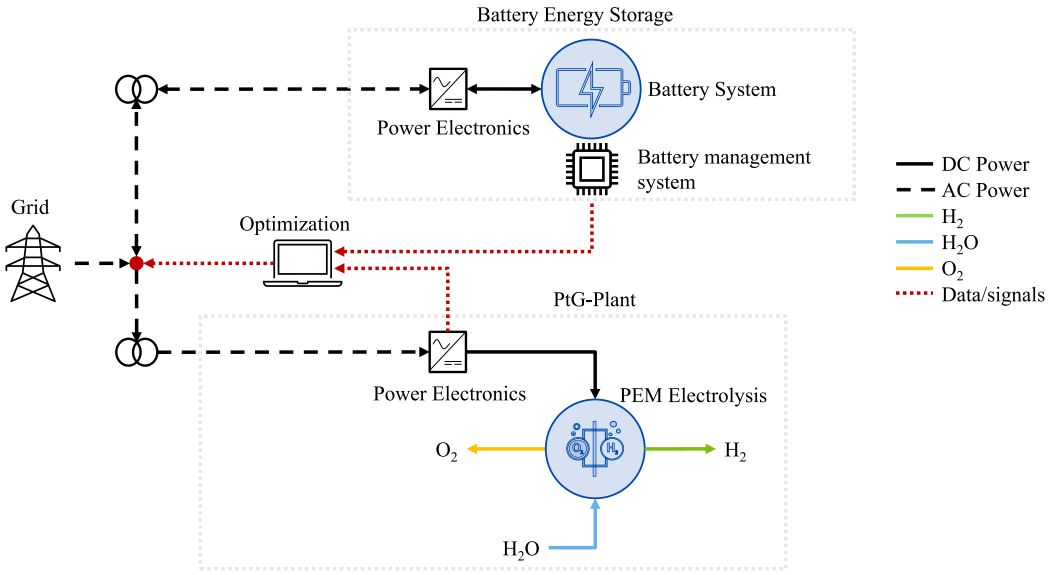


**Fig. 1.** System layout and optimization interface.

### 3.3. Battery energy storage system

Large scale BESS are very dynamic systems with time constants in the range of seconds [44,45]. Due to the considered time intervals in this work of 1 h it is not necessary to model the dynamics of the BESS in detail. The focus is primarily on the system's efficiency $\eta$ and the amount of energy that can be stored within the BESS. Therefore, the battery is modeled as a storage for the usable energy $E_{\text{Batt}} = 9\,\text{MW h}$ and available charging and discharging power. The relative amount of the usable energy by the BESS for every $k$ and the time step $\Delta t = 1\,\text{h}$ is given by

$$SOE_k = SOE_{k-1} + \frac{P_{\text{Batt},k} \cdot \Delta t \cdot \eta}{E_{\text{Batt}}}. \tag{3.2}$$

The maximum usable power at each operating point is calculated by solving Eq. (3.2) for $P_{\text{Batt}}$ with 0 as lower and 1 as upper boundary of the $SOE$. Additionally, an aging model needs to be implemented to enable the DP to optimize the operating strategy considering battery aging. Similarly to the PEMEL model calculating the number of EOH, equivalent full cycles (EFC) are determined as $QLV$ for the battery. A battery lifetime of 10,000 cycles [46] is assumed. Following the procedure for $c_{\text{QLV}}$ in Section 3.2, the costs per EFC ($c_{\text{EFC}}$) are obtained. This value is necessary to calculate the costs related to battery aging

$$C_{\text{aging,Batt}} = \frac{(F_{SOE} + F_P) \cdot |P_{\text{Batt},k}| \cdot \Delta t \cdot \eta}{2 \cdot E_{\text{Batt}}} \cdot c_{\text{EFC}}, \tag{3.3}$$

with constant $P_{\text{Batt}}$. This can be used within the minimization of the overall costs. The determination of the EFC consider stressful operating conditions for the BESS, like low or high $SOE$ ($F_{SOE}$) as well as discharging or charging the BESS with relatively high power ($F_P$). The critical operating conditions and their influence on the number of EFC are listed in Table 3.

**Table 3**
Critical operating conditions for the aging of the BESS.

| Factor | Operating condition | Value in EFC |
|---|---|---|
| $F_{SOE}$ | $SOE <= 20\ \%$ | 0.6 |
| | $20\ \% < SOE < 80\ \%$ | 0.5 |
| | $SOE >= 80\ \%$ | 0.6 |
| $F_P$ | $\lvert P_{\text{Batt}}\rvert < 70\ \%\ P_{\max}$ | 0.5 |
| | $\lvert P_{\text{Batt}}\rvert >= 70\ \%\ P_{\max}$ | 0.6 |

## 4. Implementation of the optimization algorithm

Both plants are connected to the grid and the power demand of the electrolyzer can be met by either the grid or the battery, or a combination of both. It is assumed that the grid can always supply the requested energy without constraints, since a detailed model of the electricity market is not within the scope of this paper. In this work it is assumed that the battery cannot feed into the grid, but only into the electrolyzer. Furthermore, the decision at each $k$ is considered constant for one hour.

$SOE_0$ and $SOE_N$ at the start and the end of the optimization period need to be defined with the same value in order not to falsify the results by using additional energy stored in the BESS that has not been purchased at the day-ahead market before. For this purpose the BESS is defined to be empty ($SOE = 0$) at the beginning and the end of the optimization. The influence of temperature on the systems as well as standby power consumption of the plants are neglected and $\eta$ for the BESS is considered 1.

At the intersection (see Fig. 1) between the grid, the BESS and the PEMEL the DP decides on the operating strategy and the power distribution between the components. The observation period includes the time horizon $N$ of one week with time steps $k$ of one hour. The desired target value $z_N$ is predefined for every week and must be reached after 168 h at the latest. In this paper the simulations are executed for up to $z_N = 20\,\text{t}$ resulting from the utilization target of 6,000 FLH $\text{a}^{-1}$ for the electrolyzer. One of the advantages of DP and the principle of Bellman is the possibility of deriving the solution for other target values from the generated state matrices. Therefore, in this work different $z_N$ can be considered with only one simulation. The exact values are listed in Table 4. After creating the possible solutions, the respective $z_N$ can simply be chosen as the initial value of the backward recursion to find the globally optimal trajectory. Additionally to this constraint of a desired amount of hydrogen, other conditions have to be fulfilled.

The power restrictions of the PEMEL and the battery may not be exceeded. The minimal power of the electrolyzer is set to 1.8 MW due to a stronger influence of gas crossover in the low partial-load range [47]. From the maximum power of 9 MW for the PEMEL and the BESS (positive and negative) as well as the capacity of the battery with 9 MWh result discrete power steps of 0.9 MW or fractions of that value for the decisions $x_{\text{El},k}$ and $x_{\text{Batt},k}$. They span the decision spaces $X_{\text{El},k}$ and $X_{\text{Batt},k}$ for each plant. The state space $Z_{\text{El},k}$ consists of the

**Table 4**
Parameters for the models of the Wunsiedel Energy Park.

| Parameter | PEMEL | BESS |
|---|---|---|
| Power range | 0, 1.8, 2.7, …,9 MW | −9, −8.1, …, 9 MW |
| Energy | – | 9 MW |
| $\beta_{\mathrm{P2M}}$ | $\frac{165}{9}$ kg MW$^{-1}$ | – |
| $\beta_{\mathrm{P2S}}$ | – | $\frac{1}{9}$ h MW$^{-1}$ |
| $QLV$ | 80,000 EOH | 10,000 EFC |
| $CAPEX$ | 1,000 kW$^{-1}$ | 800 kW$^{-1}$ |

possible amounts of hydrogen that can be produced in intervals of 16.5 kg corresponding to the discrete power steps of the electrolyzer.

The transfer function

$$t_{\mathrm{El},k} = z_{\mathrm{El},k-1} + x_{\mathrm{El},k} \cdot \beta_{\mathrm{P2M}} \tag{4.1}$$

connects the state at the last time step $k-1$ to the current one dependent on the decision $x_k$ and the factor $\beta_{\mathrm{P2M}}$ for the mass of produced hydrogen per MW.

For the BESS, the state space $Z_{\mathrm{Batt},k}$ contains the possible $SOE$ in the system, which can range between 0 and 1. The discrete power steps of 0.9 MW result in steps of 0.1 for $Z_{\mathrm{Batt},k}$.

The transfer function

$$t_{\mathrm{Batt},k} = z_{\mathrm{Batt},k-1} + x_{\mathrm{Batt},k} \cdot \beta_{\mathrm{P2S}} \tag{4.2}$$

clarifies the connection between battery decision and state with $\beta_{\mathrm{P2S}}$ as conversion factor.

Based on the models and electricity prices $c_{\mathrm{el},k}$ at the day-ahead market for each $k$ the objective function

$$F(x_1, \ldots, x_n) = \sum_{k=1}^{N} c_{\mathrm{el},k} \cdot (x_{\mathrm{El},k} + x_{\mathrm{Batt},k}) \cdot \Delta t + C_{\mathrm{aging},k} \tag{4.3}$$

can be formulated for the optimization problem. The term

$$C_{\mathrm{aging},k} = C_{\mathrm{aging,El},k} + C_{\mathrm{aging,Batt},k} \tag{4.4}$$

describes the economic evaluation of the aging of both components that is defined in Eq. (3.1) and (3.3) respectively. Eq. (4.3) can be optimized for different system performance parameters (SPP). These include the EPC ($C_{\mathrm{aging},k} := 0$), EOH ($c_{\mathrm{EFC}} := 0$), EFC ($c_{\mathrm{EOH}} := 0$) or EOC, where the EPC and all aging related costs are considered.

The DP then minimizes the objective function for the desired SPP. The overall structure of the optimization algorithm is depicted in Fig. 2.

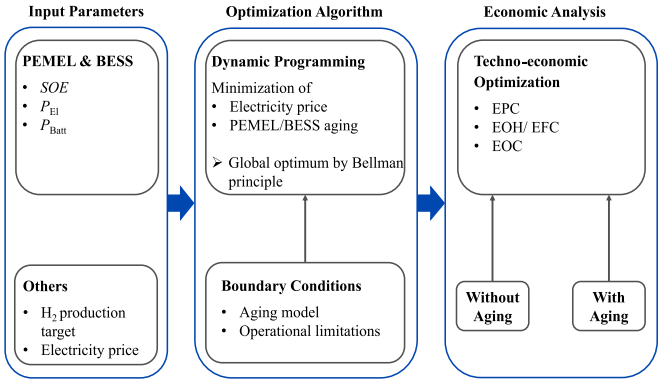


**Fig. 2.** Operating strategy optimization of the hybrid system.

## 5. Scenario definition

To demonstrate the practicability of the developed algorithm several scenarios are considered:

1. Selection of power step size
2. Investigation of the sample week in April 2021
3. Statistical evaluation of the years 2021 and 2022
4. Parameter study of $c_{\mathrm{EOH}}$ and $c_{\mathrm{EFC}}$
5. Comparison of FLH and EOH

First, the power step sizes used in the DP are varied. Since they influence both the result of the DP and the corresponding computing time, a compromise must be found when selecting the optimal step size.

The functioning of the algorithm is then illustrated as an example for the week from April 30 to May 6 in 2021. The coupled operating strategy and the corresponding SPP of the cases in Table 5 are compared with each other:

For a valid analysis of the significance of the results, a statistical evaluation of the simulations is carried out for each week of the years 2021 and 2022.

To investigate the influence of the specific aging costs on the optimization results a sensitivity analysis for $c_{\mathrm{EOH}}$ and $c_{\mathrm{EFC}}$ is conducted. Based on the assumptions in Table 4, the bold values in Table 6 and their variations for the sensitivity analysis result.

The service lifetime of electrolyzer systems is often expressed in FLH. Consequently, the final investigation of this paper includes a comparison between the accumulated FLH and EOH during an annual operation to check whether FLH is a sufficient assessment parameter.

An overview of the simulation parameters for the different scenarios can be found in Table 6. The optimization is carried out with MATLAB on a DELL Inc. Precision 3650 Tower with an Intel Xeon W-1390P 3.5 GHz processor and 128 GB RAM memory.

## 6. Results

### 6.1. Selection of the power step size

As mentioned in Section 5, the resulting computing time and the desired accuracy of the optimization algorithm need to be considered when selecting the power step size. The influence of the target value for weekly hydrogen production and the choice of the power step size for three different cases on the overall computing time is shown in Fig. 3. The computing time is highly dependent on the size of the state spaces $Z_{\mathrm{El},k}$ and $Z_{\mathrm{Batt},k}$. As the number of possible states increases, the optimization algorithm requires more time to determine the optimal solution of the minimization problem.

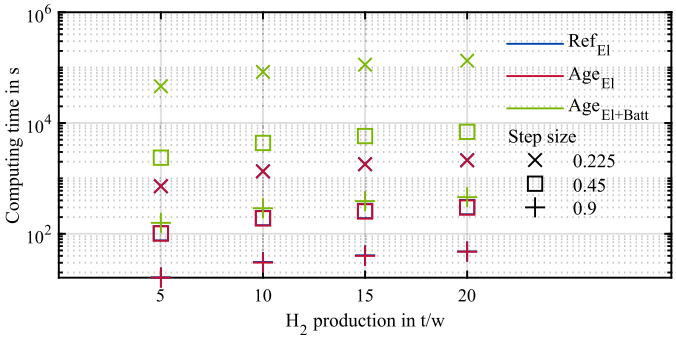


**Fig. 3.** Influence of the power step size on the computing time per simulation for different hydrogen production targets.

The increase in weekly hydrogen production leads to an expansion of the state space $Z_{\mathrm{El},k}$ and thus, to a linear increase in computing time.

Furthermore, additional states are obtained through the coupled operation of PEMEL and BESS, as distinct decisions can be made for the BESS corresponding to each decision of the PEMEL. Compared to the first two cases without BESS ($\mathrm{Ref_{El}}$ and $\mathrm{Age_{El}}$), this results in a significant extension of the computing time. The reduction of the power step size has the strongest influence on the simulation time. As the step size decreases, the computing time increases exponentially. This can once more be ascribed to the expanding number of states in both PEMEL and BESS.

**Table 5**
Scenarios and used model configurations.

| Scenario | PEMEL model | BESS model | PEMEL aging model | BESS aging model |
|---|---|---|---|---|
| $\text{Ref}_{\text{El}}$ | ✓ | – | – | – |
| $\text{Age}_{\text{El}}$ | ✓ | – | ✓ | – |
| $\text{Ref}_{\text{El+Batt}}$ | ✓ | ✓ | ✓ | – |
| $\text{Age}_{\text{El+Batt}}$ | ✓ | ✓ | ✓ | ✓ |

**Table 6**
Simulation parameters.

| Parameter | Values | Unit |
|---|---|---|
| Observation period $N$ | 168 | h |
| Target values $z_N$ | 5, 10, 15, 20 | t |
| Power step size | 0.225, 0.45, 0.9 | MW |
| Electricity prices $c_{\text{el},k}$ | day-ahead prices of 2021, 2022 [48] | $\text{MWh}^{-1}$ |
| Costs per EOH $c_{\text{EOH}}$ | 56.25, 84.375, **112.5**, 140.625, 168.75, 196.875, 225 | $\text{EOH}^{-1}$ |
| Costs per EFC $c_{\text{EFC}}$ | 180, 270, 360, 450, 540, 630, **720** | $\text{EFC}^{-1}$ |

Fig. 4 illustrates the impact of varying power step sizes on the optimization results, represented as the average EOC over the weekly hydrogen production. Compared to the computing time, the global optimum for EOC has a negligible dependence on the power step size. The maximum deviation in the EOC between a step size of 0.9 and 0.225 is smaller than 0.02%, whereas a slightly better solution is always achieved when using the smaller one. This plausibility check proves the functionality of the optimization algorithm. Since the considerable increase in computing time outweighs the advantage of the small improvement with respect to the global optimum, the step size is set to 0.9 in this work.

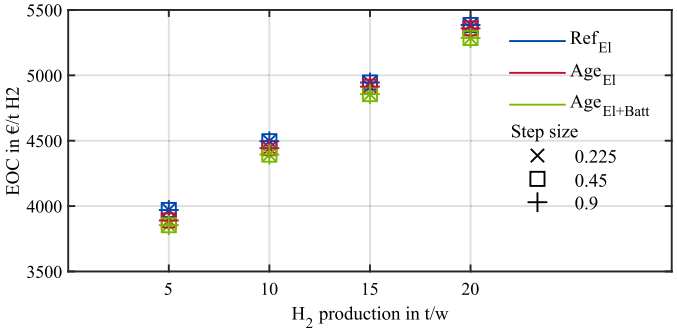


**Fig. 4.** Influence of the power step size on the EOC for different hydrogen production targets.

### 6.2. Analysis of the optimized operating strategies

To provide more insight into the functioning of the optimization algorithm, the resulting strategies for the cases defined in Table 5 are shown in Fig. 5 for the sample week in April 2021. The simulation is carried out for a target value $z_N$ of 10 t. Fig. 5 a) shows the optimized operating strategy for $\text{Ref}_{\text{El}}$. This case is a purely economic optimization regarding the EPC. For a better comparability the electricity prices of this week are plotted as well.

Without consideration of aging it is economically viable to operate the electrolyzer at the lowest prices until the specified hydrogen production target is reached. For this sample week this occurs, if the price drops below $50\,€\,\text{MWh}^{-1}$. This value for the marginal costs depends on the weekly electricity prices as well as the respective $z_N$. As the power profile is optimized without the aging model, the electrolyzer operates at maximum power at low prices and is switched off at prices exceeding the marginal costs. This results in a highly dynamical operation of the system with 20 start-stop sequences. In Fig. 6 the savings in terms of EPC, aging costs of the battery and the electrolyzer as well as EOC for the different cases in relation to the reference case explained above are depicted. Positive values mean that the optimized operating strategy of the considered case reduces the respective SPP while negative values result in an increase. In Fig. 5 b) the optimized operating strategy of $\text{Age}_{\text{El}}$ is depicted. The significant influence of the aging model is demonstrated by the less dynamic operating strategy with a more continuous mode of operation and only 6 start-stop sequences. This leads to a system operation during higher electricity prices compared to the reference case and consequently to an increase of the EPC by 1.7%. However, the accumulated costs for the EOH decrease by 13 %. The algorithm provides a strategy that, purely based on EPC, is less economically feasible in order to ensure an operation with less PEMEL aging. Thus, the overall EOC (sum of EPC, $c_{\text{aging,El}}$ and $c_{\text{aging,Batt}}$) are reduced by 4.4%. The optimized PEMEL operating strategy and the amount of electrical energy provided by the grid (Grid2El) and the BESS (Batt2El) respectively for $\text{Ref}_{\text{El+Batt}}$ are shown in Fig. 5 c). The BESS allows operation of the PEMEL during higher electricity prices and therefore the amount of start-stop sequences can be reduced to 4. Thus, by implementing the battery in the optimization $c_{\text{aging,El}}$ can be decreased by 14.5% compared to the reference case in Fig. 5 a). Additionally, the BESS ensures a more economical operation and the EPC decreases by 13 %. The operating strategy of the BESS is presented in Fig. 5 d). The power profile shows that the dynamics of the electrolyzer operation is transferred to the BESS to reduce the accumulated EOH. As the optimization of the battery strategy for this case is carried out without consideration of BESS aging the EOC increase by 0.1% compared to the reference case without battery. This case aims to maximize the EPC savings with the BESS and therefore charges the system as often as possible at low electricity prices and discharges it at high prices resulting in 18 EFC for this week. Since this case serves as reference for the one considering BESS aging, $c_{\text{aging,Batt}}$ in Fig. 6 is set to 0 to highlight the savings of the resulting operating strategies presented next. Fig. 5 e) depicts the results of the optimization of both systems considering their respective aging models. No significant changes of the resulting PEMEL operating strategy can be observed compared to Fig. 5 c) and thus $c_{\text{aging,El}}$ is exactly the same as in the case before. However, the BESS operates with lower charging and discharging powers and the number of EFC decreases significantly, resulting in a reduction of $c_{\text{aging,Batt}}$ by 60 % compared to the battery reference case. The less dynamic operation of the BESS leads to a EPC reduction of 11 % and the EOC of the complete system decreases by 6.9% compared to the reference case without battery or aging considerations. Therefore, the functionality of the optimization algorithm is clearly shown by these example cases.

### 6.3. Statistical annual evaluation

In order to obtain a more general assessment of the optimization algorithm, the results for each week of the years 2021 and 2022 are compared in an annual statistical evaluation. As illustrated in Fig. 7, electricity prices in 2022 show major differences in their course compared to 2021. Due to the energy crisis, electricity prices recorded both

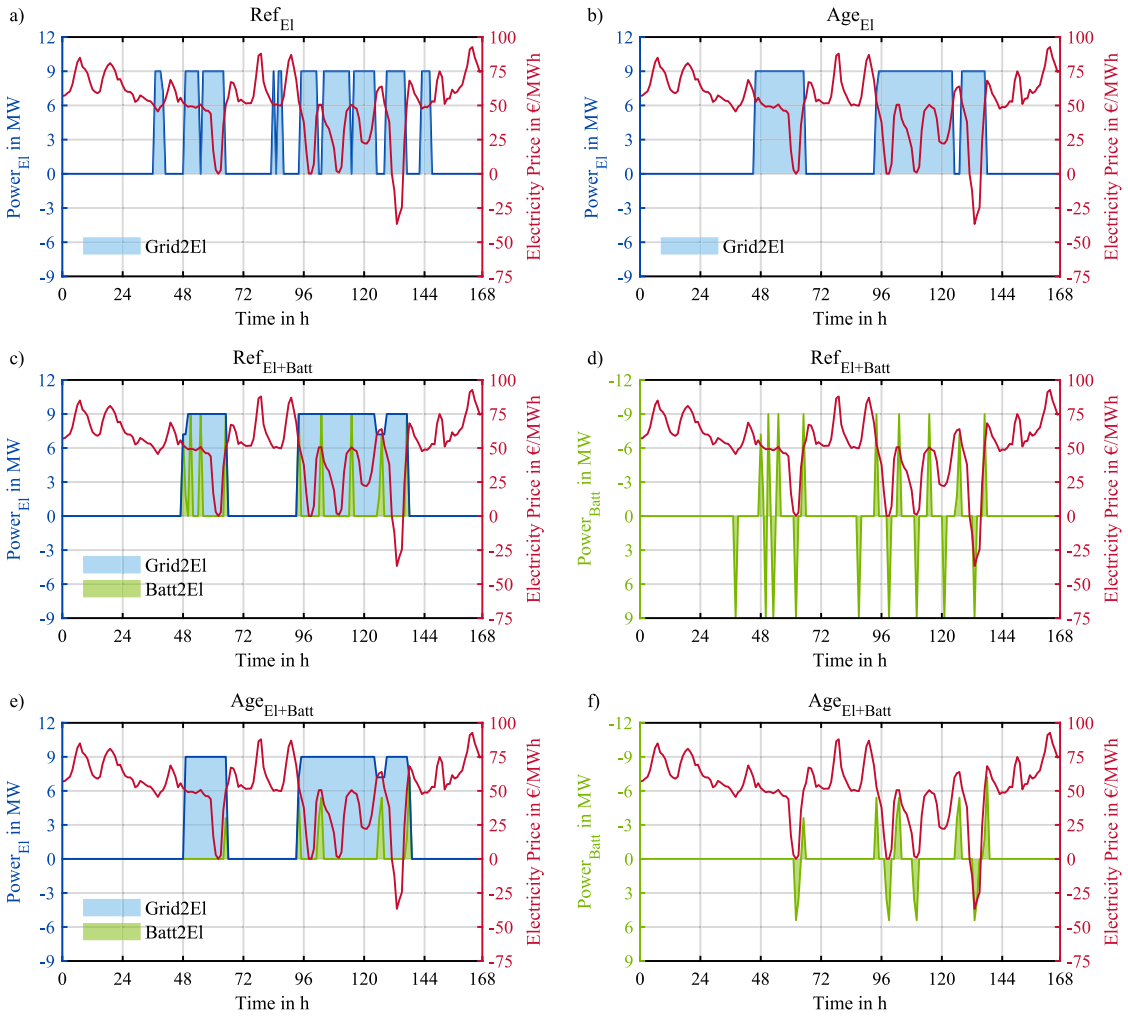


**Fig. 5.** Operating strategy for the sample week April 30 to May 6 in 2021. (a) Electrolyzer without aging, (b) electrolyzer with aging, (c) electrolyzer with aging and battery without aging, (d) battery without aging, (e) electrolyzer with aging and battery with aging, (f) battery with aging.

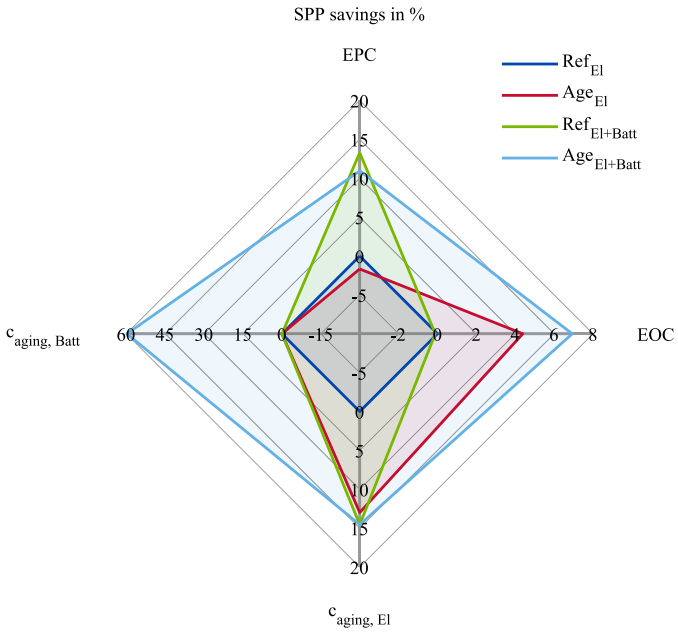


**Fig. 6.** Savings in terms of SPP in comparison to the reference case for the sample week April 30 to May 6 in 2021.

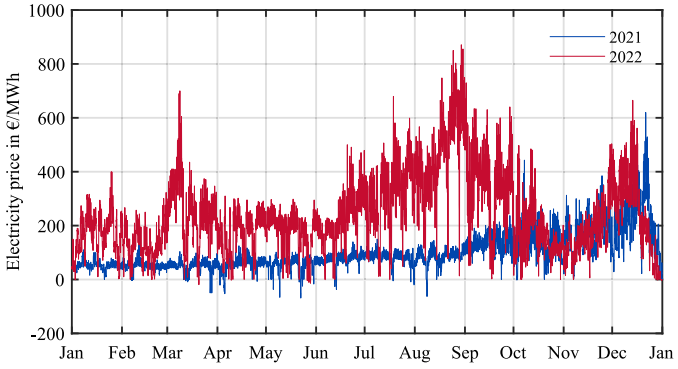


**Fig. 7.** Electricity prices of the day-ahead market for the years 2021 and 2022.

a considerably higher level and increased fluctuation. To demonstrate the influence of the electricity prices on the optimization results, the relative EOC savings of the case $\mathrm{Age_{El+Batt}}$ in relation to the reference case $\mathrm{Ref_{El}}$ for each hydrogen production target are shown as boxplots in Fig. 8. The highest relative savings can be achieved with a hydrogen production of $5\,\mathrm{t\,w^{-1}}$. This results from increasing flexibility as the target value $z_N$ decreases. Due to the higher plant utilization with increased hydrogen production, the electrolyzer must run at higher prices in order to achieve the specified hydrogen amount, which leads

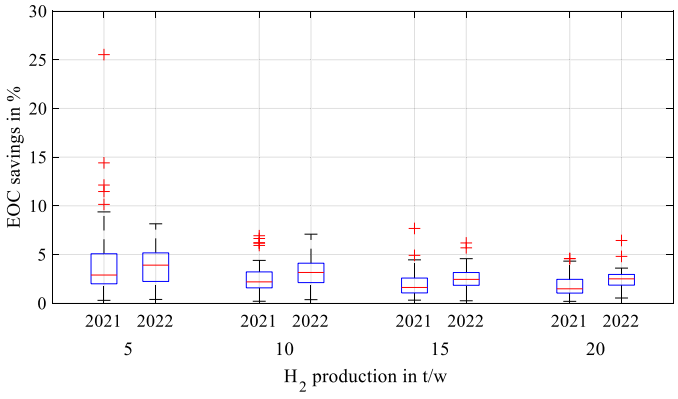


**Fig. 8.** Statistical evaluation of the simulated operating strategies for the years 2021 and 2022 at different hydrogen production targets.

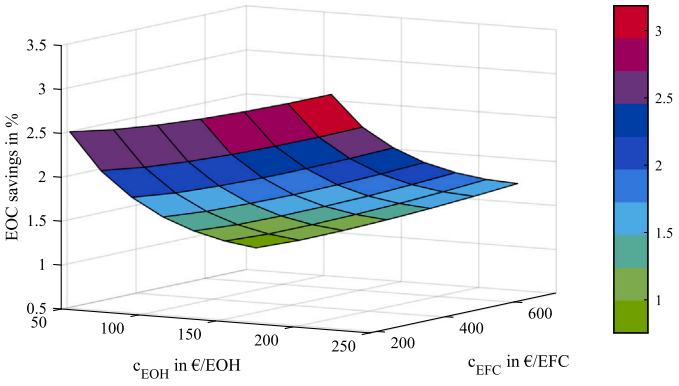


**Fig. 9.** Influence of different $c_{QLV}$ for electrolyzer and battery on the relative EOC savings.

to a reduction in cost savings. In addition, the increased electrolyzer utilization and the associated reduction in flexibility also reduce the scattering in the results of the optimization algorithm.

The sample week from Section 6.2 with EOC savings of about 7 % represents an outlier in the year 2021. Nevertheless, the operating strategy of this week is used in this paper as an example, because it provides an optimal illustration of the functionality of the algorithm. The median savings with a target value of $10\,\mathrm{t\,w^{-1}}$ in 2021 are significantly lower at around 2.2%. For a hydrogen production of $20\,\mathrm{t\,w^{-1}}$, which roughly corresponds to the future expectations of the plant operators, about 1.5% EOC savings can be achieved. However, the EOC savings correspond to an amount of about 100,000 € that a plant operator can save through an optimized operating strategy in the considered year.

The impact of the energy crisis on the electricity market shown in Fig. 7 lead to a significant enhancement of the optimization potential. Using the 2022 electricity prices, the median annual EOC savings reach a value of around 2.5% for a hydrogen production of $20\,\mathrm{t\,w^{-1}}$, which corresponds to an absolute cost reduction of around 300,000 € compared to the reference case. The overall savings potential of the developed optimization algorithm thus depends strongly on the electricity market pricing.

The statistical analysis of the optimization results proves that the EOC of the electrolyzer can be reduced with the support of the BESS. The battery has a very low utilization rate for this type of application and can be used simultaneously for further value-adding tasks, e.g. the participation in the control reserve market.

### 6.4. Parameter study of the aging models

In this section the influence of the specific aging costs $c_{QLV}$ and the aging models on the resulting operating strategies for a hydrogen production target of $20\,\mathrm{t\,w^{-1}}$ is studied and discussed. According to Eq. (2.7) the specific aging costs consist of the $CAPEX$ and the expected system lifetime. Therefore, by varying $c_{\mathrm{EOH}}$ and $c_{\mathrm{EFC}}$ different cases like cheaper or more durable components can be considered. The variation is executed according to Table 6.

Fig. 9 shows the average EOC savings of the year 2021 for the $\mathrm{Age_{El+Batt}}$ scenario compared to $\mathrm{Ref_{El}}$. It can be stated that the surface plane characterizing the overall savings is slightly curved and that the sensitivity toward the costs per EFC is minimally higher than toward its EOH equivalent. This behavior can be explained by the fact that with lower $c_{\mathrm{EFC}}$ the resulting operating strategies for the BESS lead to a higher usage of the battery and therefore less power for the electrolyzer has to be provided by the grid.

The functionality of the PEMEL aging model is demonstrated by Fig. 10. It shows that with increasing $c_{\mathrm{EOH}}$ the optimization algorithm aims to reduce the EOH more and more, while the variation of $c_{\mathrm{EFC}}$ has a negligible influence on the resulting electrolyzer profile. The same behavior for EFC savings can be identified with increasing $c_{\mathrm{EFC}}$. Thus, the generic aging model can be weighted in favor of one of the two plants depending on the chosen specific aging costs.

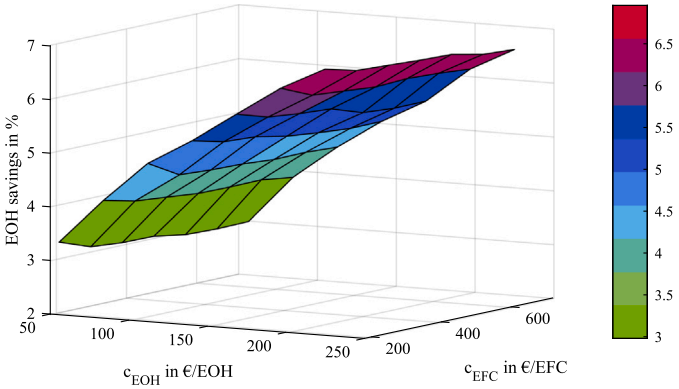


**Fig. 10.** Influence of different $c_{QLV}$ for electrolyzer and battery on the relative EOH savings.

### 6.5. Comparison of electrolyzer lifetime quantification

The quantification of the service lifetime for electrolyzers represents significant information for plant operators. Since the service lifetime is often expressed in FLH, the influence of dynamic operation behavior can thus not be captured. By using EOH, the dynamics of the electrolyzer during operation are considered and more reliable operating strategies can be developed. Fig. 11 shows the difference between the two aging quantifications for an annual operation of the electrolyzer plant for different hydrogen production targets per week in 2021.

The reference case ($\mathrm{Ref_{El}}$) and the case with coupled operation ($\mathrm{Age_{El+Batt}}$) are used for the representation of EOH. The FLH analysis is also based on the results of the reference case ($\mathrm{Ref_{El}}$). However, instead of calculating the EOH in the aging model, the FLH of the annual operation are determined based on the electrolyzer decisions $x_{\mathrm{El},k}$.

Using the optimization algorithm, the EOH during operation can be reduced by up to 7 % for a hydrogen production of $20\,\mathrm{t\,w^{-1}}$ and up to 12 % for a production of $5\,\mathrm{t\,w^{-1}}$ compared to the reference case. Assuming a service lifetime of 80,000 EOH, this corresponds to an increase in lifetime of over half a year for $20\,\mathrm{t\,w^{-1}}$ and over three years for $5\,\mathrm{t\,w^{-1}}$.

Across the entire hydrogen production, the values of the FLH are significantly lower than the EOH. With an annual utilization of 6,000 FLH, which corresponds to a hydrogen production of about $20\,\mathrm{t\,w^{-1}}$, the electrolyzer would reach the end of life after approximately 13 years

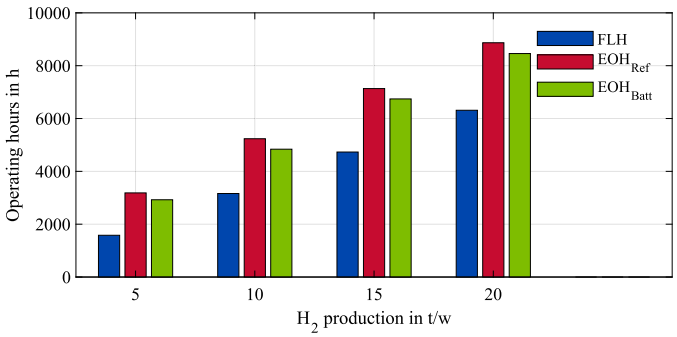


**Fig. 11.** Comparison of FLH and EOH for different hydrogen production targets in 2021.

assuming a service lifetime of 80,000 operating hours. Calculating the electrolyzer aging based on the EOH, however, results in a service lifetime of only 9 years for the reference case with the same annual hydrogen production. The comparison shows that the use of FLH as an assessment parameter can lead to a major misjudgement of the expected service lifetime of electrolyzers. Therefore, a quantification of the lifetime in EOH should be considered in order to enable a reliable prediction based on the operating dynamics.

## 7. Conclusion

In this paper an optimization algorithm based on dynamic programming has been developed providing the most economic coupled operating strategy for a grid connected hybrid system consisting of a secondary energy storage and a production plant. In contrast to the current literature shown in Section 1.2, the system degradation is considered during the optimization process and minimizes the component degradation resulting from harmful operating points. The algorithm allows optimizing the operating strategy with respect to various SPP for a predefined target value and observation period. The prerequisite for the applicability of the algorithm is full knowledge of a volatile cost profile as input parameter.

The functionality is shown for a system of a grid connected electrolyzer coupled with a battery energy storage and its system dimensions based on Wunsiedel Energy Park in Germany. The operating strategy is optimized with respect to electricity procurement costs at the day-ahead market as well as performance degradation of the hybrid system.

The results show that an improved operating strategy can decrease the effective operating costs by up to 7 % while also ensuring operating conditions for the plants with reduced degradation implications. The statistical annual evaluation of the optimization results demonstrates that the possible savings from an improved operating strategy depend strongly on the course of electricity prices.

Using FLH as an assessment parameter can lead to a considerable misjudgement of the expected service lifetime of electrolyzers as operation dynamics are neglected. Quantification of the lifetime in EOH as introduced in this work allows a more reliable prediction based on the operating dynamics.

In conclusion it can be stated that optimized operating strategies are essential for an economic and sustainable operation of hybrid systems. The algorithm developed in this paper can contribute to an optimal operation of the different players in the future energy market. In addition, the results allow the system operator to use the global optimum as a guideline for their decision making process and to choose an hourly optimized operating strategy that best suits their specific requirements. The flexibility of the developed aging model in combination with DP allows an application for a wide range of technologies and scenarios. With a precise parameterization of the aging models it is also possible to predict the required investment costs and expected lifetime of the plants for a profitable system configuration.

## CRediT authorship contribution statement

**Patrick Mößle:** Writing – original draft, Visualization, Validation, Software, Methodology, Investigation, Data curation, Conceptualization. **Tim Herrmannsdörfer:** Writing – original draft, Visualization, Validation, Software, Methodology, Investigation, Data curation, Conceptualization. **Matthias Welzl:** Writing – review & editing, Supervision, Project administration, Methodology, Funding acquisition, Conceptualization. **Dieter Brüggemann:** Supervision, Project administration, Funding acquisition. **Michael A. Danzer:** Writing – review & editing, Supervision, Project administration, Methodology, Funding acquisition, Conceptualization.

## Declaration of competing interest

The authors declare that they have no known competing financial interests or personal relationships that could have appeared to influence the work reported in this paper.

## Acknowledgment

The authors acknowledge the funding by the Oberfrankenstiftung (Upper Franconia Foundation) within the project “ZET-Reallabor Energiezukunft Wunsiedel”.

## References

[1] Yue M, Lambert H, Pahon E, Roche R, Jemei S, Hissel D. Hydrogen energy systems: A critical review of technologies, applications, trends and challenges. Renew Sustain Energy Rev 2021;146:111180. http://dx.doi.org/10.1016/j.rser.2021.111180.

[2] Yusaf T, Laimon M, Alrefae W, Kadirgama K, Dhahad HA, Ramasamy D, et al. Hydrogen energy demand growth prediction and assessment (2021–2050) using a system thinking and system dynamics approach. Appl Sci 2022;12(2):781. http://dx.doi.org/10.3390/app12020781.

[3] Ganjehsarabi H. Performance assessment of solar-powered high pressure proton exchange membrane electrolyzer: A case study for Erzincan. Int J Hydrog Energy 2019;44(20):9701–7. http://dx.doi.org/10.1016/j.ijhydene.2018.12.007.

[4] Möckl M, Bernt M, Schröter J, Jossen A. Proton exchange membrane water electrolysis at high current densities: Investigation of thermal limitations. Int J Hydrog Energy 2020;45(3):1417–28. http://dx.doi.org/10.1016/j.ijhydene.2019.11.144.

[5] Stansberry JM, Brouwer J. Experimental dynamic dispatch of a 60 kW proton exchange membrane electrolyzer in power-to-gas application. Int J Hydrog Energy 2020;45(16):9305–16. http://dx.doi.org/10.1016/j.ijhydene.2020.01.228.

[6] Zhao D, Xia Z, Guo M, He Q, Xu Q, Li X, et al. Capacity optimization and energy dispatch strategy of hybrid energy storage system based on proton exchange membrane electrolyzer cell. Energy Convers Manage 2022;272:116366. http://dx.doi.org/10.1016/j.enconman.2022.116366.

[7] Lange H, Klose A, Lippmann W, Urbas L. Technical evaluation of the flexibility of water electrolysis systems to increase energy flexibility: A review. Int J Hydrog Energy 2023;48(42):15771–83. http://dx.doi.org/10.1016/j.ijhydene.2023.01.044.

[8] Grigoriev SA, Fateev VN, Bessarabov DG, Millet P. Current status, research trends, and challenges in water electrolysis science and technology. Int J Hydrog Energy 2020;45(49):26036–58. http://dx.doi.org/10.1016/j.ijhydene.2020.03.109.

[9] Shiva Kumar S, Himabindu V. Hydrogen production by PEM water electrolysis – A review. Mater Sci Energy Technol 2019;2(3):442–54. http://dx.doi.org/10.1016/j.mset.2019.03.002.

[10] Nguyen T, Abdin Z, Holm T, Mérida W. Grid-connected hydrogen production via large-scale water electrolysis. Energy Convers Manage 2019;200:112108. http://dx.doi.org/10.1016/j.enconman.2019.112108.

[11] Mucci S, Mitsos A, Bongartz D. Power-to-X processes based on PEM water electrolyzers: A review of process integration and flexible operation. Comput Chem Eng 2023;175:108260. http://dx.doi.org/10.1016/j.compchemeng.2023.108260.

[12] Kopp M, Coleman D, Stiller C, Scheffer K, Aichinger J, Scheppat B. Energiepark Mainz: Technical and economic analysis of the worldwide largest Power-to-Gas plant with PEM electrolysis. Int J Hydrog Energy 2017;42(19):13311–20. http://dx.doi.org/10.1016/j.ijhydene.2016.12.145.

[13] Jorgensen C, Ropenus S. Production price of hydrogen from grid connected electrolysis in a power market with high wind penetration. Int J Hydrog Energy 2008;33(20):5335–44. http://dx.doi.org/10.1016/j.ijhydene.2008.06.037.

[14] Ghaebi Panah P, Cui X, Bornapour M, Hooshmand R-A, Guerrero JM. Marketability analysis of green hydrogen production in Denmark: Scale-up effects on grid-connected electrolysis. Int J Hydrog Energy 2022;47(25):12443–55. http://dx.doi.org/10.1016/j.ijhydene.2022.01.254.

[15] Papadopoulos V, Desmet J, Knockaert J, Develder C. Improving the utilization factor of a PEM electrolyzer powered by a 15 MW PV park by combining wind power and battery storage – Feasibility study. Int J Hydrog Energy 2018;43(34):16468–78. http://dx.doi.org/10.1016/j.ijhydene.2018.07.069.

[16] Gillessen B, Heinrichs HU, Stenzel P, Linssen J. Hybridization strategies of power-to-gas systems and battery storage using renewable energy. Int J Hydrog Energy 2017;42(19):13554–67. http://dx.doi.org/10.1016/j.ijhydene.2017.03.163.

[17] Alia SM, Stariha S, Borup RL. Electrolyzer durability at low catalyst loading and with dynamic operation. J Electrochem Soc 2019;166(15):F1164–72. http://dx.doi.org/10.1149/2.0231915jes.

[18] Wallnöfer-Ogris E, Grimmer I, Ranz M, Höglinger M, Kartusch S, Rauh J, et al. A review on understanding and identifying degradation mechanisms in PEM water electrolysis cells: Insights for stack application, development, and research. Int J Hydrog Energy 2024;65:381–97. http://dx.doi.org/10.1016/j.ijhydene.2024.04.017.

[19] Parra D, Patel MK. Techno-economic implications of the electrolyser technology and size for power-to-gas systems. Int J Hydrog Energy 2016;41(6):3748–61. http://dx.doi.org/10.1016/j.ijhydene.2015.12.160.

[20] Matute G, Yusta JM, Beyza J, Correas LC. Multi-state techno-economic model for optimal dispatch of grid connected hydrogen electrolysis systems operating under dynamic conditions. Int J Hydrog Energy 2021;46(2):1449–60. http://dx.doi.org/10.1016/j.ijhydene.2020.10.019.

[21] Torreglosa JP, García P, Fernández LM, Jurado F. Hierarchical energy management system for stand-alone hybrid system based on generation costs and cascade control. Energy Convers Manage 2014;77:514–26. http://dx.doi.org/10.1016/j.enconman.2013.10.031.

[22] García P, Torreglosa JP, Fernández LM, Jurado F. Optimal energy management system for stand-alone wind turbine/photovoltaic/hydrogen/battery hybrid system with supervisory control based on fuzzy logic. Int J Hydrog Energy 2013;38(33):14146–58. http://dx.doi.org/10.1016/j.ijhydene.2013.08.106.

[23] Zhou L, Song A, Zhou Y. Electrification and hydrogenation on a PV-battery-hydrogen energy flexible community for carbon–neutral transformation with transient aging and collaboration operation. Energy Convers Manage 2024;300:117984. http://dx.doi.org/10.1016/j.enconman.2023.117984.

[24] Ibáñez-Rioja A, Järvinen L, Puranen P, Kosonen A, Ruuskanen V, Hynynen K, et al. Off-grid solar PV–wind power–battery–water electrolyzer plant: Simultaneous optimization of component capacities and system control. Appl Energy 2023;345:121277. http://dx.doi.org/10.1016/j.apenergy.2023.121277.

[25] Maluenda M, Córdova S, Lorca Á, Negrete-Pincetic M. Optimal operation scheduling of a PV-BESS-electrolyzer system for hydrogen production and frequency regulation. Appl Energy 2023;344:121243. http://dx.doi.org/10.1016/j.apenergy.2023.121243.

[26] Palm H, Holzmann J. Hyper space exploration a multicriterial quantitative trade-off analysis for system design in complex environment. In: 2018 IEEE international systems engineering symposium. IEEE; 2018, p. 1–6. http://dx.doi.org/10.1109/SysEng.2018.8544435.

[27] Mößle P, Tietze T, Danzer MA. Kalman filter tuning for state estimation of lithium–Ion batteries by multi–objective optimization via hyperspace exploration. Energy Technol 2023;11(12). http://dx.doi.org/10.1002/ente.202300796.

[28] Floudas CA, Lin X. Mixed integer linear programming in process scheduling: modeling, algorithms, and applications. Ann Oper Res 2005;139(1):131–62. http://dx.doi.org/10.1007/s10479-005-3446-x.

[29] Chen S, Hu M, Guo S. Fast dynamic-programming algorithm for solving global optimization problems of hybrid electric vehicles. Energy 2023;273:127207. http://dx.doi.org/10.1016/j.energy.2023.127207.

[30] Bellman R. Dynamic programming, In: Princeton landmarks in mathematics, 1st ed., Princeton Landmarks in Mathematics ed., with a new introduction. Princeton, NJ: Princeton University Press; 2010.

[31] Bellman R. Dynamic programming. Science 1966;153(3731):34–7. http://dx.doi.org/10.1126/science.153.3731.34.

[32] Domschke W, Drexl A, Klein R, Scholl A. Einführung in operations research, In: Lehrbuch, 9th ed., überarbeitete und verbesserte Auflage. Berlin and Heidelberg: Springer Gabler; 2015, http://dx.doi.org/10.1007/978-3-662-48216-2, URL http://www.springer.com/.

[33] Li J, Danzer MA. Optimal charge control strategies for stationary photovoltaic battery systems. J Power Sources 2014;258:365–73. http://dx.doi.org/10.1016/j.jpowsour.2014.02.066.

[34] Marano V, Rizzo G, Tiano FA. Application of dynamic programming to the optimal management of a hybrid power plant with wind turbines, photovoltaic panels and compressed air energy storage. Appl Energy 2012;97:849–59. http://dx.doi.org/10.1016/j.apenergy.2011.12.086.

[35] Papageorgiou M, Leibold M, Buss M. Optimierung. Berlin, Heidelberg: Springer Berlin Heidelberg; 2015, http://dx.doi.org/10.1007/978-3-662-46936-1.

[36] Rüther T, Mößle P, Mühlbauer M, Bohlen O, Danzer MA. Iterative dynamic programming—An efficient method for the validation of power flow control strategies. Electricity 2022;3(4):542–62. http://dx.doi.org/10.3390/electricity3040027.

[37] Cormen TH. Introduction to algorithms. 3rd ed. Cambridge, Mass.: MIT Press; 2009.

[38] Zhang S, Sun XA. Stochastic dual dynamic programming for multistage stochastic mixed-integer nonlinear optimization. Math Program 2022;196(1–2):935–85. http://dx.doi.org/10.1007/s10107-022-01875-8.

[39] Zou B, Peng J, Li S, Li Y, Yan J, Yang H. Comparative study of the dynamic programming-based and rule-based operation strategies for grid-connected PV-battery systems of office buildings. Appl Energy 2022;305:117875. http://dx.doi.org/10.1016/j.apenergy.2021.117875.

[40] Russell SJ, Norvig P. Artificial intelligence: A modern approach, In: Always learning, 3rd ed., Global edition. Boston: Pearson; 2016.

[41] Kleinberg J, Tardos E. Algorithm design: pearson new international edition. 1st ed., Auflage. Harlow: Pearson Education Limited; 2013, URL https://elibrary.pearson.de/book/99.150005/9781292037042.

[42] Belenguer E, Segarra-Tamarit J, Pérez E, Vidal-Albalate R. Short-term electricity price forecasting through demand and renewable generation prediction. Math Comput Simulation 2025;229:350–61. http://dx.doi.org/10.1016/j.matcom.2024.10.004.

[43] Fritz DL, Mergel J, Stolten D. PEM electrolysis simulation and validation. ECS Trans 2014;58(19):1–9. http://dx.doi.org/10.1149/05819.0001ecst.

[44] Eskandari M, Rajabi A, Savkin AV, Moradi MH, Dong ZY. Battery energy storage systems (BESSs) and the economy-dynamics of microgrids: Review, analysis, and classification for standardization of BESSs applications. J Energy Storage 2022;55:105627. http://dx.doi.org/10.1016/j.est.2022.105627.

[45] Brogan PV, Best RJ, Morrow DJ, McKinley K, Kubik ML. Effect of BESS response on frequency and RoCoF during underfrequency transients. IEEE Trans Power Syst 2019;34(1):575–83. http://dx.doi.org/10.1109/TPWRS.2018.2862147.

[46] Jasper FB, Späthe J, Baumann M, Peters JF, Ruhland J, Weil M. Life cycle assessment (LCA) of a battery home storage system based on primary data. J Clean Prod 2022;366:132899. http://dx.doi.org/10.1016/j.jclepro.2022.132899.

[47] Schalenbach M, Carmo M, Fritz DL, Mergel J, Stolten D. Pressurized PEM water electrolysis: Efficiency and gas crossover. Int J Hydrog Energy 2013;38(35):14921–33. http://dx.doi.org/10.1016/j.ijhydene.2013.09.013.

[48] FraunhoferISE. Energy-charts. 2024, URL https://www.energy-charts.info/index.html?l=de&c=DE. [Accessed 06 February 2024].